NIKOLA M. NIKAČEVIĆ

ALEKSANDAR P. DUDUKOVIĆ

Department of Chemical Engineering, Faculty of Technology and Metallurgy, University of Belgrade, Belgrade, Serbia

FLUID DYNAMICS OF GAS – FLOWING SOLIDS – FIXED BED CONTACTORS

Fluid dynamics studies of countercurrent gas – flowing solids – fixed bed contactors are presented in this review. The up–to–date research findings about the basic fluid dynamics parameters: flowing solids holdup, pressure drop and flow pattern are reviewed. Experimental results, as well as theoretical studies and mathematical models are observed and commented.

Key words: Gas – flowing solids – fixed bed contactors, Multiphase reactors, Flowing solids holdup, Pressure drop, Residence time distribution

In this type of equipment fine solids particles and gas are flowing countercurrently (or cocurenntly) through the column which is packed with the other solids phase. In the literature such columns are named "gas – flowing solids – fixed bed contactors", or "raining packed bed contactors", or "solids trickle flow contactors".

The concept of contacting gas and fine solids particles (flowing solids) inside a packed bed was patented nearly sixty years ago [1]. The first realization occurred in France for heat recovery, and since then other applications were under consideration. They include separation processes, drying and heat exchange, etc. These contactors can be applied for novel types of equipment with integrated and coupled processes. The examples would be catalytic chemical reactors with adsorption in situ and integrated processes with heterogeneous chemical reaction and simultaneous heat exchange in a bed of catalyst.

First studies of countercurrent flow of gas and fine solids particles inside the packed bed were carried out by Kaveckii and Plankovskii [2]. In later studies researchers paid considerable attention to the fluid dynamics of such systems [3–30], as well as to heat and mass transfer [6–8,31–36]. Westerterp and colleagues [37–40] proposed the use of fine solids as a regenerative adsorbent, which flows through the bed of catalyst in the case of methanol synthesis. Similar approaches can be found in the work of Verver [6] and Verver and Van Swaaij [41], who investigated catalytic oxidation of hydrogensulfide, as well as in the work of Kiel [10] and Kiel, Prins and Van Swaaij [42] who studied regenerative desulfurization of flue gases. Comprehensive survey of investigations regarding applications

as well as heat and mass transfer in gas – flowing solids – fixed bed contactors can be found in the book chapter by Duduković and Nikačević [43].

The first industrial gas – flowing solids – fixed bed heat exchanger, commercially named "Saturne", was developed by French company Saint–Gobain and one of its subsidiaries TNEE [31,34]. The TNEE application has been used for the thermal reclaiming of foundry sands. In order to avoid high energy consumption, two gas – flowing solids – fixed bed heat exchangers were integrated with a fluidized bed combustion unit (Fig. 1). The industrial operating unit has confirmed the experimental data obtained through both laboratory and pilot tests. This specially designed system operates with zero supplemental fuel consumption when used sand contains more than 1% of organic compounds.

Gas – flowing solids – fixed bed contactors can be considered as two phase or three phase systems. In the first case, gas and flowing solids are the contacting phases, while the packing only enables better contact between the flowing phases. In that case there are no limitations in geometry and design of packing elements. In the second case, the packing elements are third
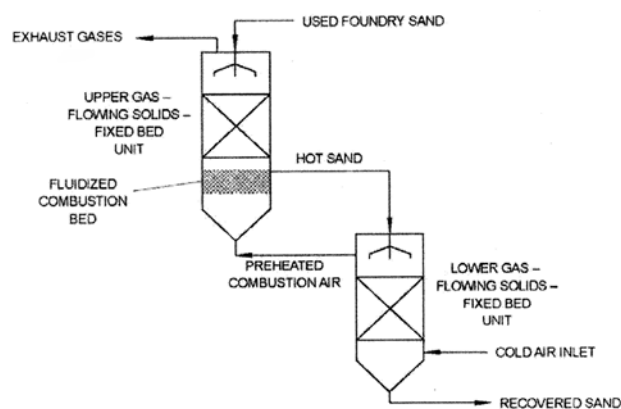
Figure 1. Foundry sand reclamation system consisting of two gas – flowing solids – fixed bed heat exchangers and a combustion fluidized bed. Conceptual design [34].

active phase, as in heterogeneous catalytic reactors. In these cases the geometry of packing elements is limited by the process requirements, i.e. by the shape of catalyst particles.

In this review fluid dynamics of countercurrent gas – flowing solids – fixed bed contactors will be presented. The up–to–date research findings of basic fluid dynamics parameters: flowing solids holdup, pressure drop and flow pattern are reviewed.

FLOWING SOLIDS HOLDUP AND VELOCITIES

Flowing solids holdup represents the volume of flowing solids per unit bed volume and it is usually divided into two parts: dynamic and static holdup. The latter represents the fraction of flowing solids particles that rest on the packing elements. After shutting down the flowing solids and gas inlets, these particles that constitute static solids holdup, remain in the bed. Dynamic holdup represents the fraction of flowing solids that is suspended in the gas stream between the packing elements. These fine solid particles flow out after the inlets of gas and flowing solids are closed.

Experimental Results

Similar to gas – liquid systems, in gas – flowing solids – fixed bed countercurrent contactors three regimes were observed: preloading, loading and flooding. At low gas flow rates (preloading), gas essentially does not affect the flow of solids, and consequently, flowing solids dynamic holdup is nearly independent of gas flow rate. At higher gas flow rates (loading regime) gas slows down the flow of solids, and there is a strong interaction between the gas flow and flowing solids. In the loading regime dynamic holdup increases with a gas velocity. In Fig. 2 a typical behavior of dynamic holdup as a function of gas flow rate is presented.

If gas flow rate is further increased, the relative velocity between the gas and flowing solids approaches the value of the terminal velocity. The flowing solids phase starts to accumulate in the upper part of the packing, and these unstable conditions are called flooding. Flooding is characterized with sudden, sharp increase in both pressure drop and dynamic holdup. This regime, which should be avoided, was registered in many of the laboratory and pilot–plant scale experiments. However, in some of industrial scale experiments, in columns of large diameter, there was no flooding, but instead a distinct segregation of gas and flowing solids flows occurred [8].

A number of experimental studies on determination of dynamic holdup were carried over the years, using columns of different constructions and dimensions, a variety of packing elements and flowing solids with a wide range of mean diameters and properties. In Table 1 the sources of experimental data are reviewed together with basic information on experimental conditions in their experiments. The ranges of obtained data for dynamic holdup are presented in Fig. 3.

Static holdup was not intensively studied, because it plays a minor role in the efficiency of the column, and because the technique for its determination is more complicated and time consuming. Geometry of packing elements has a major influence on static holdup. Flowing solids physical properties also significantly influence static holdup. Solids flow rate also has some
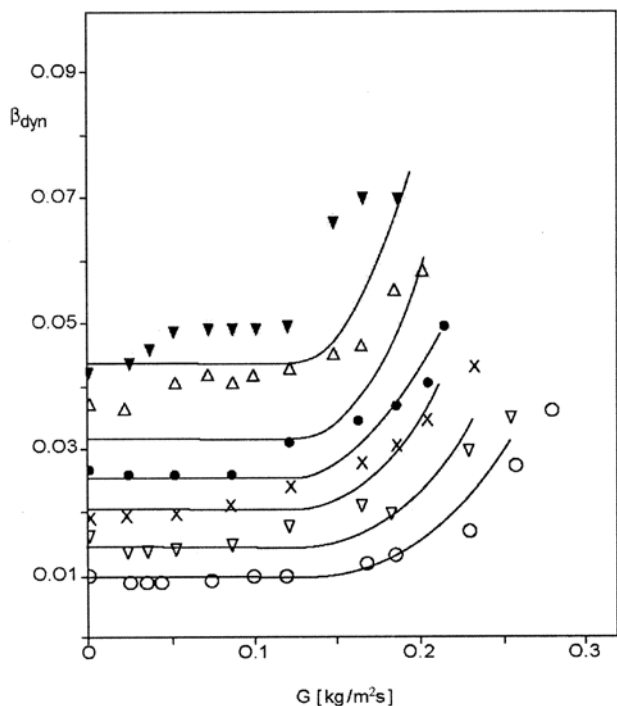
Figure 2. Typical results for dynamic holdup in gas – flowing solids – fixed bed contactors. Dynamic holdup as a function of superficial gas velocity for different values of flowing solids flow rates. Different symbols correspond to different flowing solids mass fluxes in the range 1.32 – 6.13 kg/m^{2}s [4].
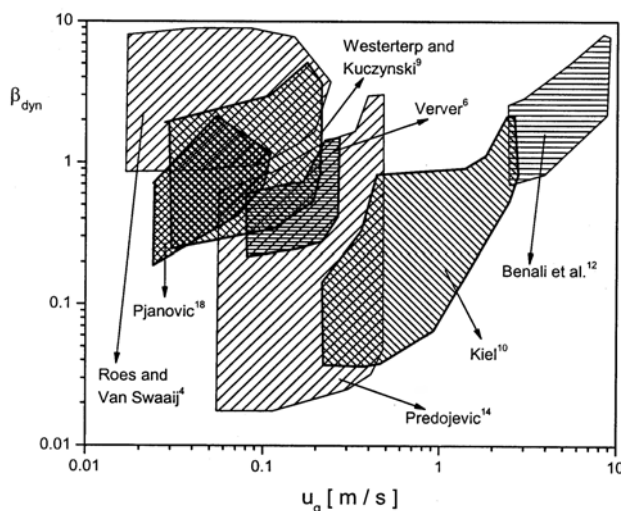
Figure 3. Survey of the experimental results for dynamic holdup as a function of superficial gas velocity [43].

Table 1. Studies of the Fluid Dynamics in Gas – Flowing Solids – Fixed Bed Contactors

	Column diameter [m]	Packing type and size	[mm]	Void fraction of packing	Flowing solids phase: type and size [μm]		Solid mass flux [kg/m²s]	Superficial gas velocity [m/s]
Kaveckii, and Planovskii [2]	0.127	Raschig rings,	15*15	0.64	silicagel,	366	0.14–0.56	0.16–0.46
Claus et al. [3]	0.092	cylindrical screens,	20*20	0.97	sand,	235	9–42	0.02–1.7
Roes and Van Swaaij [4]	0.076	Raschig rings, Pall rings, cylindrical screans,	10*10*1 15*15*2 10*10*0.5	0.80 0.86 0.97	FCC,	70	1.1–6.0 1.3–6.0 1.3–6.0	0.02–0.19 0.02–0.23 0.02–0.17
Large et al. [5]	0.32	Pall rings,	15*15	0.94	sand,	190	0.66–1.68	0.22–1.72
Saatdjian and Large [7]	0.125	Pall rings,	15*15	0.93	sand,	205	0–3	0–4
Verver and Van Swaaij [8]	0.10*0.10	regulary stacked packing,	15*15		FCC, sand, sand, steel shot, steel shot,	70 255 425 310 880	0.03–0.8 0.1–2.4 0.2–2.2 0.3–4.8 0.3–4.0	0–0.2 0–0.9 0–1.4 0–2.8 0–5.4
Westerterp and Kuczynski [9]	0.025	Raschig rings, kerapak,	7*7*3	0.45 0.75	FCC,	80	0.5–2.0	0.03–0.16 0.03–0.26
Kiel [10]	10*10	regulary stacked packing,	3	0.61	glas beads, glas beads,	490 740	0.1–1 0.43–1	0.2–1 0.5–1
Predojević [14]	0.111	Raschig rings, Raschig rings, cer. beads, Pall rings, Raschig rings, Raschig rings, cer. beads, Pall rings,	12*12*2.4, 30*30*2.3 19 23*8*0.1 12*12*2.4 30*30*2.3 19 23*8*0.1	0.61 0.85 0.47 0.96 0.61 0.85 0.47 0.96	sand, propant,	253 642	0.16–2.5 0.14–2.5	0.06–0.46
Stanimirović [17]	0.111	Raschig rings, cer. beads, Raschig rings, cer. beads, Raschig rings, cer. beads,	12*12*2.4 19 12*12*2.4 19 12*12*2.4 19	0.61 0.47 0.61 0.47 0.61 0.47	semolina, sand, corundum,	348 253 331	0.07–1.09 0.18–2.6 0.23–3.46	0.12–0.46
Pjanović [18]	0.0274	glass beads, glass beads, Raschig rings,	5 6 5*5	0.41 0.44 0.71	poliamid,	105	0.12–0.13 0.12–0.58 0.13–0.58	0.02–0.12

influence on static holdup, as it increases with solids flux [14]. According to some authors [8,14] the static holdup is essentially independent of gas flow rate. However, other authors [12] found a slight increase of static holdup with gas flow rate, though an explanation for such phenomenon was not offered. Typical results [14], representing the influence of gas velocity, solids flux and packing type on static holdup, are presented in Fig. 4.

Mathematical models

The development of phenomenological models, in order to describe the fluid dynamics of the gas – flowing solids – fixed bed contactors, was the objective of a numerous studies [4, 6, 8–10, 20–25]. Due to very complex interactions in these systems, fluid dynamic behavior is still under investigation. Some of the phenomena occurring are difficult to describe rigorously,
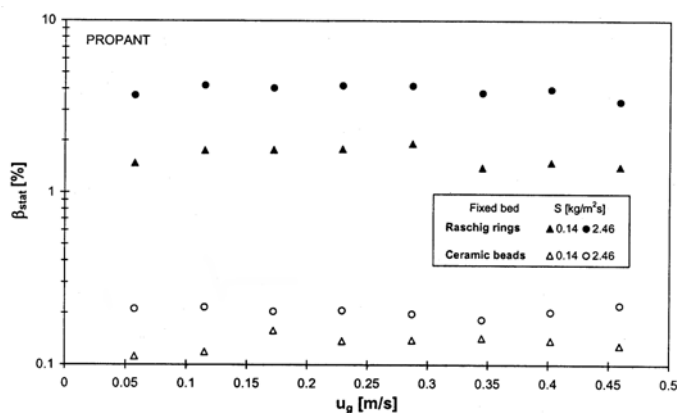

Figure 4. Typical results for static holdup in gas – flowing solids – fixed bed contactors. Static holdup in two different fixed beds, as a function of superficial gas velocity for different values of flowing solids fluxes [14]

so models proposed up–to–date are based on a number of simplifications, and most of them contain empirical parameters.

Countercurrent flow of gas and flowing solids inside the packed bed has some analogies with gas – liquid systems, as preloading, loading and flooding regimes. However, in many aspects the nature of these phenomena are different and equations for gas – liquid systems can not be applied to flowing solids systems.

a) Empirical Correlations

Empirical correlations for prediction of dynamic holdup in countercurrent gas – flowing solids contactors were offered. Correlations are based on the experimental data available in the literature, and consequently can not be recommended for extrapolations.

According to their empirical analysis, Nikačević, Duduković and Predojević [20] proposed two different dynamic holdup expressions, one for preloading and the other for loading regime. The dynamic holdup (β_{dyn}) in the preloading regime can be calculated from the following dimensionless equation [20]:

$$\beta_{dyn} = 2.196 \cdot 10^3 \cdot Re^{1.21} \cdot Ar^{-0.88} \cdot \left(\frac{S^2}{\rho_s \cdot \rho_g \cdot u_g^2} \right)^{0.582} \cdot$$

$$\cdot (d_s / d_{eq})^{2.41} \cdot (1 - \varepsilon)^{1.42} \cdot \varepsilon^{0.279} \quad (1)$$

where Re is particle Reynolds number.

For the loading regime it was obtained [20]:

$$\beta_{dyn} = 15.57 \cdot 10^3 \cdot Re^{1.57} \cdot Ar^{-1.24} \cdot \left(\frac{S^2}{\rho_s \cdot \rho_g \cdot u_g^2} \right)^{0.509} \cdot$$

$$\cdot (d_s / d_{eq})^{2.93} \cdot (1 - \varepsilon)^{1.46} \cdot \varepsilon^{-1.45} \quad (2)$$

This concept requires prediction of fluid dynamic regime before equations (1) and (2) can be used. A criterion, which was used in this analysis, was based on the Reynolds number at the loading point, i.e. at the transition from preloading to loading regime [19]:

$$Re_{load} = 0.1289 \cdot Ar^{0.48} (d_s/d_{eq})^{-1.11} \cdot (G/S)^{0.23} \cdot \varepsilon^{0.85} \quad (3)$$

Alternatively, dynamic holdup can be predicted by the single equation, independently of the regime [20]:

$$\beta_{dyn} = 6.561 \cdot 10^3 \cdot Re^{1.29} \cdot Ar^{-1.01} \cdot \left(\frac{S^2}{\rho_s \cdot \rho_g \cdot u_g^2} \right)^{0.521} \cdot$$

$$(d_s/d_{eq})^{2.57} \cdot (1 - \varepsilon)^{1.52} \cdot \varepsilon^{0.933} \quad (4)$$

Equation (4) is convenient as it does not require prior determination of the regime, and it gives an average error of 26.9% for the loading regime, which is very close to the error of equation (2), being 26.4% (based on 270 available loading data points). However, the difference in errors between predicted and experimental data for the preloading regime is higher for equation (4), than for equation (1) by about 8%.

b) Average Solids and Slip Velocities

The average flowing solids particle velocity can be defined as:

$$\overline{u}_s = \frac{S}{\beta_{dyn} \rho_s} \quad (5)$$

while the mean relative velocity between flowing solids and gas (slip velocity) in countercurrent systems is:

$$\overline{u}_R = \overline{u}_s + \dot{u}_g = \frac{S}{\beta_{dyn} \rho_s} + \frac{G}{(\varepsilon - \beta) \rho_g} \quad (6)$$

where $\beta = \beta_{dyn} + \beta_{st}$ is total flowing solids holdup.

For the preloading regime, Roes and Van Swaaij [4] found that the average particle velocity is independent of gas and flowing solids flow rates. A constant value of average particle velocity in preloading zone was found to be 0.17 m/s in their experiments (three types of packing: Pall rings, Raschig rings and cylindrical screens). When the value of the average particle velocity is known, the value of the dynamic holdup for the preloading regime can be found from eq. (5). However, it is reasonable to assume that the mean particle velocity will depend on packing properties, and so $\overline{u}_s$ has to be determined from separate experiments for each type of packing.

Roes and Van Swaaij [4] concluded from their experiments for the loading regime that under these conditions the relative (slip) velocity is constant, having the value of 0.31 m/s. The physical reasons for this constant value of slip velocity were not discussed. In fact, it was experimentally determined later [9] that relative velocity depends on the properties of both flowing phases, as well as on the packing geometry.

c) Trickle Flow Model

Westerterp and Kuczynski [9] approximated the flow of solids as a flow of rivulets (trickles) rather than of individual particles. They assumed that in the preloading regime the solids phase flows almost exclusively in the form of trickles. It was further assumed that some gas is dragged along by the trickles flowing downwards. The trickles release the gas when they collide with the walls of fixed bed elements. The released gas flows upwards together with the main stream and in that way local circulation of gas is produced. After collision, the stream of particles slides over the packing surface, and than again starts falling by gravity, voids in trickles are increasing and a new portion of gas is captured and dragged downwards. The distance between collisions depends on the geometry of the packing, and the mean solids velocity is the average between the velocity of falling and sliding trickles over the packing surface. Accordingly, the increase in pressure drop is caused by

trickles for two reasons: (1) the reduction of free cross section available for gas flow, due to the presence of trickles, and (2) the recirculation of gas which increases the upward gas flow.

The void fraction occupied by gas in solids trickles was introduced and defined as:

ε_{tr} = gas volume in trickles/total trickle volume

which was assumed to be constant. The real gas velocity, according to this approach is:

$$u_{g,corr} = \frac{\dfrac{G}{\rho_g} + \dfrac{S}{\rho_s} \cdot \dfrac{\varepsilon_{tr}}{1-\varepsilon_{tr}}}{\varepsilon - \beta_{st} \dfrac{\rho_s}{\rho_{s,PB}} - \dfrac{S}{\rho_s u_s (1-\varepsilon_{tr})}} \qquad (7)$$

The upward gas flow is increased by the second term in the numerator, while the free cross sectional area available for flow is reduced by the static solids holdup and the trapped gas (second term in denominator) and by the area occupied by trickles (third term in denominator). The use of real gas velocity, defined by eq. (7), in the Ergun equation allows the determination of ε_{tr} by comparison between calculated and experimental results for pressure drop. Westerterp and Kuczynski [9] have found high values for ε_{tr}, around 0.975 for their experimental conditions.

The dynamic holdup in the preloading regime was successfully predicted using this approach [9], but the empirical parameter ε_{tr} had to be determined from the same experimental data. Westerterp and Kuczynski [9] did not derive a relation for reliable prediction of dynamic holdup in the loading range. Instead, for rough estimation the use of equations (5) and (7) was suggested.

d) Particle Flow Model

In countercurrent gas – flowing solids systems dynamic holdup (i.e. the volumetric solids concentration) usually has low values, as seen from Fig. 3. Consequently, in first approximation, solids flow can be considered as a sum of single particle flows. In these systems, particles repeatedly collide with the packing, which retards their motion, causing a higher residence time of the flowing solids. The relative velocity between particles and gas does not usually reach the terminal velocity. The acceleration of the particles in the downward direction through the gas flowing upward is given by the momentum equation:

$$\rho_s \frac{du_s}{dt} = F_G - F_B - F_D \qquad (8)$$

where F_G, F_B, and F_D are gravitational, buoyancy and drag forces per unit solids volume, and u_s is the local particle velocity in the downward direction:

$$u_s = \frac{dz}{dt} \qquad (9)$$

Equation (8) in describing particle motion is applicable for the period between two successive collisions with packing elements.

Verver and Van Swaaij [8] and Kiel and Van Swaaij [23] introduced the concept of a "packing cell" for regularly stacked packing. In this approach, regularly stacked packing is considered as a two–dimensional array of identical packing cells and the fluid dynamic modeling is restricted to a single cell. Duduković, Nikačević and Kuzeljević [25] considered flowing particles behavior in an "average void" as representative of a whole bed, for both random and regular packings.

The flowing solids – packing interaction was taken into account through the initial solids velocity in the vertical direction, at the entrance of the packing cell, or the packing void. In some of the approaches [8,23] the initial solids velocity is treated as an empirical factor which had to be determined from the experiments. The other solution [25] was to assume the initial velocity to be zero, i.e. on average the particles upon collision loose all of their velocity in downward direction. Analysis by Kiel [10] proved that the values of initial velocity are small, both positive and negative, and dependant on packing geometry and flowing solids flow rate.

The forces in the eq. (8) are given by:

$$F_G - F_B = (\rho_s - \rho_g)\, g \qquad (10)$$

and

$$F_D = C_D \frac{3\rho_g}{4d_s}(u_s + u_g')^2 \qquad (11)$$

where u_g' is the mean gas velocity in the voids:

$$u_g' = \frac{u_g}{\varepsilon - \beta} = \frac{G}{(\varepsilon - \beta)\,\rho_g} \qquad (12)$$

This value of u_g' was additionally corrected by some authors [8, 23] in order to account for the nonuniformity of packing porosity and for the wakes that packing elements produce in the gas stream, especially in organized packing with free space between the packing elements. Verver and Van Swaaij [8] introduced an "effective packing porosity", while Kiel and Van Swaaij [23] defined an "effectiveness factor". Both of these empirical parameters have to be determined from experimental data.

The drag coefficient in eq. (13) is a function of the particle Reynolds number based on relative velocity:

$$Re_s = \frac{\rho_g d_s (u_s + u_g')}{\mu} \qquad (13)$$

For calculation of the drag coefficient the equation proposed by Turton and Levenspiel [26] can be used:

$$C_D = \frac{24}{Re_s}(1 + 0.173\,Re_s^{0.6567}) + \frac{0.413}{1 + 16300\,Re_s^{-1.09}} \qquad (14)$$

or some other similar equation.

e) Dynamic Holdup Predictions

The average dynamic flowing solids holdup can be found from eq. (5):

$$\beta_{dyn} = \frac{S}{\overline{u}_s \, \rho_s} \qquad (15)$$

if the average solids velocity for the "average void" or "packing cell", $\overline{u}_s$, is known.

Most of the proposed models for prediction of $\overline{u}_s$ [8,23–25] are based on the balance of the forces, explicitly given by the solution of differential equations (8) and (9). Some of the particular assumptions were mentioned in this text, but are specified in more details in the original papers together with numerical methods. In some models, empirical parameters involved were obtained by trial and error method based on experimental results [8, 23].

Verver and Van Swaaij [8] demonstrated a good agreement between calculated and experimentally determined values of average particle velocity ($\overline{u}_s$). However, their model included two empirical parameters (the effective bed void, and initial velocity) which acquired different values for each of the flowing solids materials tested. Kiel and Van Swaaij [23] found optimal values to be –0.05 m/s for initial velocity and 1.35 for effectiveness factor.

Duduković, Nikačević, Petrović and Predojević [24] introduced an empirical parameter (ψ) to take into account the acceleration of particles, and their collisions with bed elements, instead of solving equations (8) and (9). Accordingly, the average velocity was given as:

$$\overline{u}_s = \psi \cdot u_{s,t} \qquad (16)$$

where the terminal velocity is found from:

$$u_{s,t} = u_{R,t} - u_g' = \sqrt{\frac{4 d_s g \, (\rho_s - \rho_g)}{3 \rho_g C_D}} - \frac{G}{\rho_g \, (\varepsilon - \beta)} \qquad (17)$$

The empirical parameter ψ in eq. (17) does not need to be experimentally determined for each case, as it can be evaluated from a correlation given by eq. (18):

$$\psi = 0.4186 \sqrt{\frac{\rho_g}{\rho_s} \cdot \frac{d_V}{d_s}} + 0.0042 \qquad (18)$$

where d_V is the equivalent void diameter, defined as:

$$d_V = \frac{2 d_{eq}}{3 \, (1 - \varepsilon)} \qquad (19)$$

d_{eq} being equivalent packing diameter. The agreement between predicted and experimental values was good, considering a very wide range of experimental conditions used in available literature data [24]. An average error was 20.8% for 452 data points.

Models proposed by Verver and Van Swaaij [8] and Kiel and Van Swaaij [23] are semi–empirical in nature, based exclusively upon experimental data taken in a single study and were not tested on data of other authors. The model proposed by Duduković et al. [24] is semi–empirical as well, but it introduces a correlation (ψ), which allows the prediction of dynamic holdup without any experiments in a system of interest.

As an alternative to the previous approach, Duduković, Nikačević and Kuzeljević [25] proposed a model free of any empirical parameters, involving a number of simplifying assumptions. The goal was to find the particle velocity as a function of vertical distance along the void, by solving simultaneously equations (8–14). An average particle velocity can be found for the whole void, if the shape of the void is known and mathematically described. However, the geometry of the voids depends on the type of packing, and it differs in configuration and orientation even in the same bed. In order to obtain a solution which would be of general applicability, an "average void" was simply described as a vertical double cone with diameter and height equal to the average void diameter (d_V). Furthermore, the average particle velocity was found as a mean integral value for a whole void, allowing estimation of dynamic holdup by the use of eq. (15). The comparison of predicted and experimental values, based on 564 data points from the literature, led to the average discrepancy of 31.3%. This could be considered as very good agreement, taking into account a wide range of experimental conditions in both preloading and loading regimes, as well as fundamental approach with no empirical parameters involved.

PRESSURE DROP

Another important design parameter for gas – flowing solids – fixed bed contactors is pressure drop. In these multiphase contactors it originates from two major causes: flow of gas through porous media, i.e. resistance of packing elements, and drag due to interactions of flowing solids and gas. Pressure drop depends on the solids flux and gas velocity, as it can be seen in Fig. 5 for typical results. In preloading regime pressure drop increases slightly with a gas velocity, while in loading zone this raise is faster. Fig. 6 presents ranges of measured pressure drops in different investigations. Surveys, along with explanations, are presented in Table 1. According to the experiments, the general conclusion would be that values of pressure drop in this type of equipment are not as high as they can be in other gas–solids systems.

Predojević, Petrović and Duduković [19] proposed empirical correlation for pressure drop along the packed bed. Two separate equations, one for preloading and the other loading regime were offered [19], together with equation (3) for separation of data into regimes.

The pressure drop per unit bed height in the preloading regime can be found from [19]:

$$\Delta p/L = 3.057 \cdot Re^{0.44} \, Ar^{-0.19} \, Fr^{0.12} \, (d_{eq}/D)^{-1.13} \cdot$$

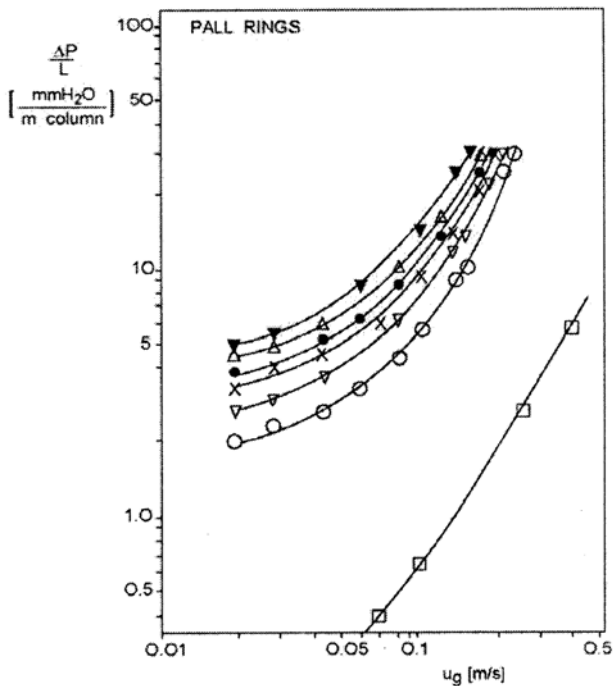$$\cdot \, (1-\varepsilon)^{0.51} \, \varepsilon^{-2.41} \qquad (20)$$

Figure 5. Typical results for pressure drop in gas – flowing solids – fixed bed contactors. Pressure drop as a function of superficial gas velocity for different values of flowing solids flow rates. Different symbols correspond to different flowing solids mass fluxes in the range 0 – 6.13 kg/m²s. (Square symbols are for S = 0) [4]
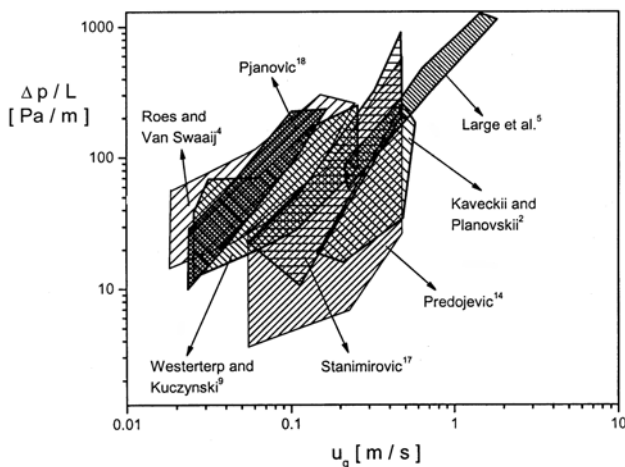

Figure 6. Survey of the experimental results for pressure drop as a function of superficial gas velocity [43].

where Fr is dimensionless Froude number for flowing solids. For loading regime the following equation was offered [19]:

$$\Delta p/L = 3.528 \cdot Re^{0.49}\, Ar^{-0.18}\, Fr^{0.1}\, (d_{eq}/D)^{-1.35} \cdot$$

$$\cdot (1-\varepsilon)^{0.51}\, \varepsilon^{-2.41} \tag{21}$$

In phenomenological approach, the usual [8,10, 23,24] simplified assumptions rest on the additivity of two pressure drop contributions given by:

$$\frac{\Delta p}{L} = \left(\frac{\Delta p}{L}\right)_{PB} + \left(\frac{\Delta p}{L}\right)_{FS} \tag{22}$$

where $\left(\dfrac{\Delta p}{L}\right)_{PB}$ is the contribution of gas – packed bed interactions, while $\left(\dfrac{\Delta p}{L}\right)_{PB}$ is the contribution of gas – flowing solids interaction in the voids. The first term can be found from the Ergun equation:

$$-\left(\frac{\Delta p}{L}\right)_{PB} = \left(\frac{A}{Re_{PB}} + B\right) \cdot \frac{u_g\, \rho_g}{d_{eq}} \cdot \frac{1 - \varepsilon_{corr}}{\varepsilon_{corr}^3} \tag{23}$$

where $\varepsilon_{corr} = \varepsilon - \beta$ and Re_{PB} is the Reynolds number for gas flow through the packed bed:

$$Re_{PB} = \frac{u_g\, \rho_g\, d_{eq}}{\mu\, (1 - \varepsilon_{corr})} \tag{24}$$

It was recommended [9, 24] that constants A and B in the Ergun equation should be determined for each packing separately, from experiments with single gas flow.

Some authors [8, 23] found it convenient to define a relative pressure drop, γ, as a ratio of the drag force exerted by the solids on the gas, and the gravity force on the solids [23]:

$$\gamma = \frac{F_D}{\beta \rho_s g} \tag{25}$$

In this approach [23] it is assumed that particle velocity varies along the packing cell, and consequently the drag force is changing. The average relative pressure $\bar{\gamma}$ can be found by integration. The predicted values of the average relative pressure drop agreed well with experimental results of Kiel and Van Swaaij [23] for the same values of empirical parameters determined for dynamic holdup. However, the error for pressure drop data was higher than for dynamic holdup, approximately by a factor of two.

Starting from equation (22), Duduković, Nikačević, Petrović and Predojević [24] predicted pressure drop caused by the flowing solids, using the value of dynamic holdup, obtained previously by the model proposed in the same work [24]. The second term in eq. (22) was derived from the drag force which acts over each flowing particle, and in summary can be calculated according to:

$$\left(\frac{\Delta p}{L}\right)_{FS} = \frac{3}{4} \cdot \frac{C_D\, \beta_{dyn}\, \rho_g\, \bar{u}_R^2}{(\varepsilon - \beta)\, d_S} \tag{26}$$

where C_D is modified drug coefficient which takes into account blockage effects of packing [24]. Their predictions were compared with 435 literature data point, giving an average error of 40.1%.

FLOW PATTERN

It is well known that plug flow is a desirable flow pattern in countercurrent separations. Real equipment always deviates from this ideal, due to the occurrence of axial (and radial) mixing. The result of this deviation is the reduction of the driving force for heat and mass transfer. Consequently, the residence time distribution (RTD) of both flowing phases in gas–flowing solids–fixed bed contactors plays an important role in the design of equipment.

For the flowing solids phase, residence time distribution curve is affected by the nature of the solids holdup. The dynamic holdup was assumed to be the operating holdup, and the static holdup was often treated as a "dead" part of flowing solids. However, if a static holdup is not inactive, and it exchanges particles with a dynamic holdup, this would affect the residence time distribution of flowing solids, and consequently overall contactor performance.

Exchange between Dynamic and Static Flowing Solids

Duduković, Nikačević, Pjanović and Kuzeljević [27] applied tracer technique to study the dynamic behavior of static particles which are temporarily settled on the packed elements. A step signal in the inlet of the flowing solids was produced by switching from powder of one color to the other (all other properties being the same). At different time intervals after a step signal, flows of gas and flowing solids were closed simultaneously, and flowing solids were drained out (dynamic part), leaving behind the stagnant portion of the solids particles. The content of the column was discharged and sieved in order to separate the stagnant flowing particles from the packing elements. The color analysis was performed in order to determine the mean value of the tracer fraction in static holdup at the certain time after the step input. These experiments were repeated for different time intervals, giving the fraction of tracer in the static part of the column as a function of time. Typical experimental results [27] are presented in Fig. 7. The exchange between stagnant and dynamic parts of flowing solids is obvious from Fig 7. However, a fraction of tracer does not reach its maximum value of one after a long time, implying that a part of stagnant particles behave as a dead zone, not taking part in the exchange. From Fig. 7 it could be estimated that, for the experimental conditions employed, the dead zone occupied about 20% of the stagnant zone [27].

Defining the flowing solids volumetric exchange rate per unit bed volume (f), the balance for the active part of the stagnant zone was given as:

$$(\beta_{st} - \beta_{dead}) V_c \frac{d\varphi}{dt} = v_{in} - v_{out} = f \cdot V_c (1 - \varphi) \quad (27)$$
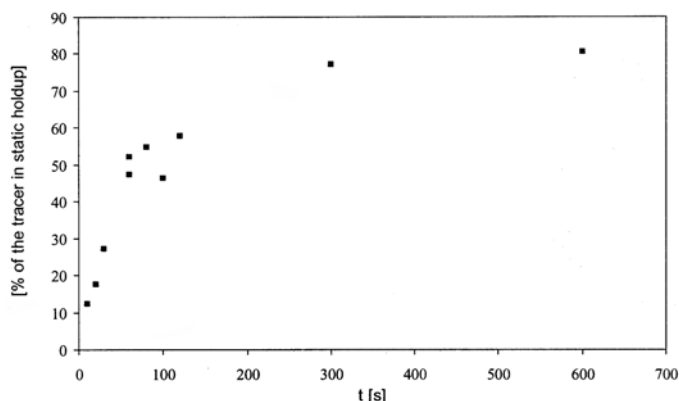

Figure 7. Exchange between dynamic and static portion of flowing solids. The percentage of tracer in static holdup as a function of time [27].

It was assumed that, after the step signal, all the particles of dynamic holdup are tracer ones (because the front moves very fast in comparison to the studied exchange phenomena). On the other hand, the flow of particles from the stagnant zone contains both tracer and inert particles, i.e. φ fraction. Fraction φ refers to the active part of the stagnant zone, while ϕ refers to the whole stagnant zone. If φ is replaced by ϕ, according to

$$\varphi (\beta_{st} - \beta_{dead}) V = \phi \cdot \beta_{st} V \quad (28)$$

Solution of equations (27, 28) is:

$$\phi = \left(1 - \frac{\beta_{dead}}{\beta_{st}}\right)\left(1 - e^{\frac{f}{\beta_{st} - \beta_{dead}}t}\right) \quad (29)$$

The logarithmic plot of equation (29) gives a straight line, and the exchange rate (f) can be determined from the slope. For their experimental conditions, and polyamide particles, Duduković et al. [27] found $f = 0.274 \cdot 10^{-3}$ m³/m³s. Nikačević and Duduković [28, 44] repeated experiments for glass and alumina as flowing particles, and equation (29) was efficiently applied to determine exchange rates. Somewhat discrepancy between model and experiments for alumina particles, suggested that behavior of static particles is more complex than how it was represented by the simple, single mixed zone approximation [28, 44].

Residence Time Distribution

Roes and Van Swaaij [29] used tracer technique to determine the residence time distribution and to measure the axial mixing in both flowing phases. The axially dispersed model was used to describe the degree of back mixing.

Imperfect pulse technique was applied [29, 30] to study the residence time distribution in the gas phase. Helium was injected in the air stream at the entrance and tracer concentration was determined in the exit stream. At zero solid mass flux (i.e. no flowing solids in the system), the Bodenstein number ($Bo_g = u_g d_s / D_g \varepsilon$)

was found to be close to the value of 2, so that the height of one Pall rings layer corresponds to a single ideally mixed unit [29, 30].

In countercurrent gas – flowing solids system, it was found that already a very small solids flow rate significantly increases gas phase dispersion. However, the Bodenstein number increases again with flowing solids rate, i.e. the axial dispersion, D_g, reduces again. The Bodenstein number is also rising with gas flow rate (Fig. 8). For the conditions of practical importance, axial dispersion is higher than in single gas flow, and layers of the 2 – 5 Pall rings are equivalent to a single mixing unit.
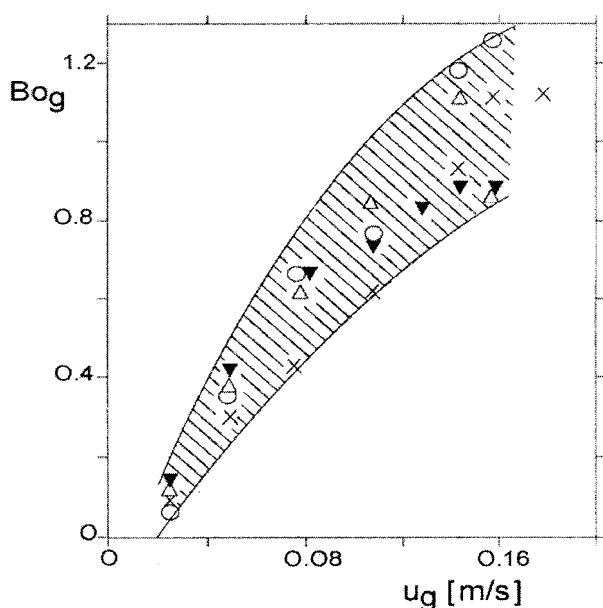

Figure 8. Axial dispersion in the gas phase. Range of Bodenstein numbers as a function of superficial gas velocity. Different symbols correspond to different values of flowing solids mass fluxes in the range 0.081 – 5.83 kg/m^{3}s [29].

Roes and Van Swaaij [29] investigated the residence time distribution of the flowing solids phase using the tracer technique, with white and black particles. A special solids tracer injector was constructed and the concentration of black particles in the exit stream was measured by a reflection technique.

Experiments demonstrated that the Bodenstein number for the flowing solids phase ($Bo_s = U_s d_s/D_s\beta$) increase with solids flow rate. On the other hand, it was found that Bos was almost independent of the gas flow rate. Near the flooding point the raise of axial dispersion in the flowing solids phase was registered. In Fig. 9 the range of Bodenstein number, as a function of the flowing solids mass flux (obtained for different values of gas flow rate), is presented. For practical conditions, 5 – 15 Pall ring layers correspond to a perfect mixing unit [29, 30].

It should be noted that in the work of Roes and Van Swaaij [29, 30] two differently defined flowing solids holdups were used. Beside the total solids holdup, the
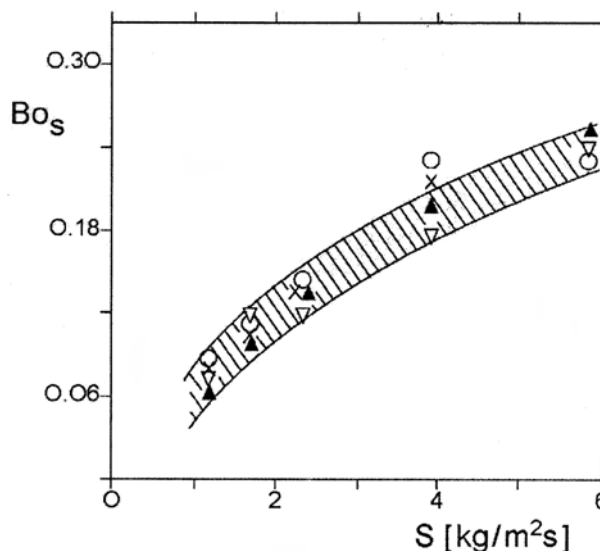

Figure 9. Axial dispersion in the flowing solids phase. Range of Bodenstein numbers as a function of flowing solids mass flux. Different symbols correspond to different values of superficial gas velocity in the range 0 – 0.130 m/s [29].

corrected one was used, which excluded that fraction of flowing solids which was named by the authors as "permanent fraction of static holdup". This fraction was experimentally determined by vibrating the column, after stopping the inlet streams and after drainage of dynamic solids. It was assumed that this fraction behaved like a part of the packing. Corrected solids holdup was in much better agreement with the results of tracer analysis. The "permanent fraction of static holdup" defined by Roes and Van Swaaij [29] and the "dead part of the static zone" defined by Duduković et al. [27] probably describe the same phenomenon, but they might not be identical.

However, experimentally obtained "long tails" of RTD curves could not be explained by the axially dispersed model proposed by Roes and Van Swaaij [29]. Nikačević and Duduković [28] considered that residence time of the flowing particles combines the residence time of suspended, fast moving particles, and the residence time of particles which spend part of the time resting on the packing elements. Experimental investigation with glass and alumina flowing particles was performed in a bench scale system in order to obtain RTD curves. Similar to the exchange experiments (described above), particles of a different color represented a tracer for the step change. The step response curves (F) were obtained by the color analysis of digital photographs. The color intensity profile was stored in a sample tube at the outlet representing "frozen" response. Color intensity of particles was related to the fractions of tracer via the calibration curve.

In order to describe complex RTD curves obtained experimentally, Nikačević and Duduković [28] proposed phenomenological model schematically presented in
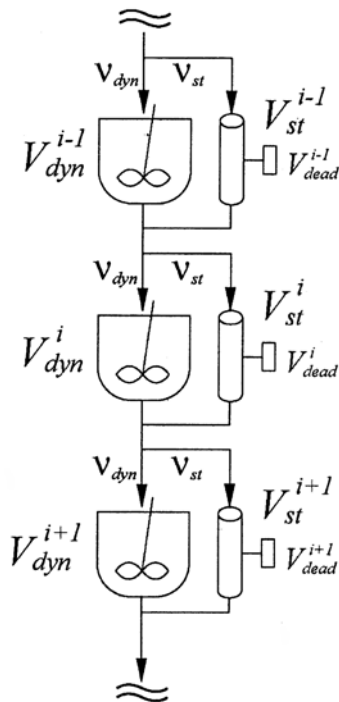
Figure 10. Schematic for the compartmental solids flow model [28].

Fig. 10. The main stream of flowing solids (dynamic holdup) is represented with a tanks–in–series model, corresponding to the degree of axial mixing. To take into account the time delay which comes from settled particles (static holdup), a parallel plug flow region was added to each of the mixing units. The authors assumed that the time delay for plug flow region represents the mean residence time of particles while settled on the packing. The portion of static holdup, which is not taking part in the exchange, was represented with "dead" volume. The model equations were derived from the material balance for one non–ideal mixing unit (i):

$$V_{dyn}^{i} \frac{dx_{dyn}^{i}(t)}{dt} = v_{dyn} \, x^{i-1}(t) - v_{dyn} \, x_{dyn}^{i}(t) \qquad (30)$$

$$x_{st}^{i}(t) = x^{i-1}(t - \tau_{st}^{i}) \qquad (31)$$

$$v_{dyn} \, x_{dyn}^{i}(t) + v_{st} \, x_{st}^{i}(t) = v \, x^{i}(t) \qquad (32)$$

where x_{dyn}^{i} and x_{st}^{i} are volumetric fractions of tracer particles: in the ideally mixed unit i, and at the exit of the plug flow unit i, respectively.

Using the Laplace technique, authors derived the equation for the step response curve (for N compartments) [28]:

$$F = \sum_{k=0}^{N-1} \binom{N}{k} y_{dyn}^{N-k} \, y_{st}^{k} \left[1 - e^{-(N\theta_{dn} - k\theta_R)} \cdot \sum_{m=0}^{N-k-1} \frac{(N\theta_{dyn} - k\theta_R)^m}{m!} \right] \cdot$$

$$\cdot \, H \, (N\theta_{dyn} - k\theta_R) + y_{st}^{N} \, H \, (N\theta_{dyn} - N\theta_R) \qquad (33)$$
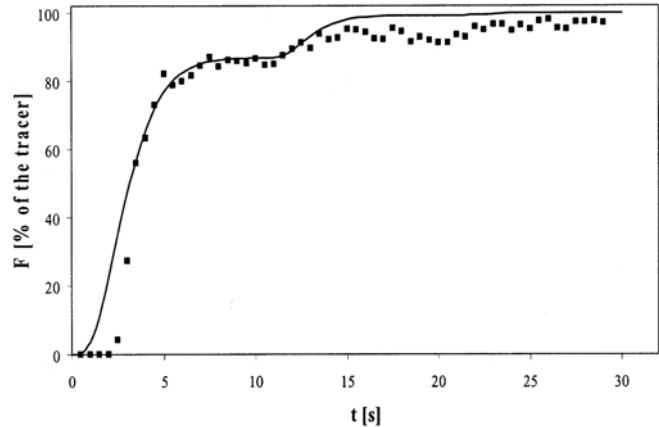

Figure 11. Residence time distribution of the flowing solids phase – response curve on a step change experiment for alumina particles. Comparison between experimentally obtained results (point symbols) and the solids flow model results (line) [28].

One could note that the response obtained from equation (33) represent the weighted sum of the responses of N tanks in series; (N–1) tanks in service with time lag τ_s/N; (N–2) tanks in series with time lag $2\tau_{st}/N$; etc. and finally plug flow response with time lag. This model was integrated with an exchange model described above [27], in order to determine parameter – time delay of static particles (τ_{st}).

Results demonstrated that, for the glass particles, one mixing unit corresponds to 8 layers of packing elements, while one mixing unit corresponds to 12 packing layers for alumina particles [28]. These results agreed with previous investigations of Roes and Van Swaaij [29, 30], where the range of 5–15 layers of packing elements were determined to behave as one mixing unit (but with packed bed consisting of Pall rings, not solid spheres).

For alumina particles, the comparison of the model and experimental results [28] is presented in Fig. 11, showing a satisfactory agreement between results. It is visible that the model predicts somewhat higher degree of axial mixing. Slight waves can be noticed in the response curve, as well. It can be presumed that these disparities are the consequence of the fact that the flow model consists of a finite (and small) number of mixing units. The other reason could be the assumption that all exchange between dynamic and static particles occurs between consecutive tanks only. Consequently, model which assumes continual exchange (at every point of the column) and predicts axial dispersion more precisely, would be more appropriate, and will be a subject of a further research.

CONCLUSSIONS

Gas – flowing solids – fixed bed contactors can be considered as equipment for a wide range of processes, as they exhibit favorable features: low pressure drop,

high mass and heat transfer rates, low axial dispersion in both flowing phases and simple construction.

Flowing solids holdup, which is usually divided into dynamic and static part, is one of the most important factors of a contactor performance. Dynamic holdup was investigated extensively and many models for its prediction can be found in the literature, along with the models for prediction of average solids velocity. On the other hand, static holdup was not investigated sufficiently, so there is a need for experimental data, as well as for mathematical models.

Pressure drop in gas – flowing solids – fixed bed contactors is generally low in comparison to the other gas – flowing particles systems. Models presented in literature can predict pressure drop with tolerable error, but one should be concerned that they may produce error of around 40%.

Flow pattern in both phases is close to a plug. The deviation is more evident for a flowing solids phase and it is a consequence of axial mixing of the fast moving particles (dynamic) and the presence of static particles which are exchanging with dynamic solids. However, part of static particles is not taking part in the exchange and it represents a "dead" zone. The influence of operational conditions on the flow pattern should be investigated in more details. Proposed models should be improved to predict a flow pattern more precisely.

ACKNOWLEDGMENTS

NOMENCLATURE

A,B constants in Ergun equation, eq. (23)

Ar   Archimedes number for flowing solids particles $(=d_s^3 \cdot (\rho_s - \rho) \cdot \rho \cdot g/\mu^2)$

Bp_g gas phase Bodenstein number $(= u_g d_s/D_g \varepsilon)$

Bo_s solids phase Bodenstein number $(=U_s d_s/D_s \beta)$

C_D drag coefficient

C_D' modified drug coefficient

D   column diameter, m

D_g gas phase axial dispersion coefficient, m^2/s

D_s solids phase axial dispersion coefficient, m^2/s

d_{eq} equivalent diameter of packing $(= 6(1-\varepsilon)/(a+4/D))$, m

d_s flowing solids particle diameter, m

d_V equivalent diameter of voids, eq. (19), m

F   step response curve – fraction of tracer particles as a function of time

F_B buoyancy force per unit solids volume, N/m^3

F_D drag force per unit solids volume, N/m^3

G_G gravity force per unit solids volume, N/m^3

Fr   Froude number for flowing solids, $(=S/\rho_s^2 g d_{eq})$

f rate of exchange between dynamic and static holdup per unit bed volume, $m^3/m^3 s$

G   gas mass flux, $kg/m^3 s$

g   gravity acceleration, m/s^2

H   Heaviside function

L   fixed bed height, m

N   number of unit compartments in solids flow model

Re   particle Reynolds number $(=u_g d_{eq}\rho_g/\mu)$

Re_{load} Reynolds number at preloading–loading transition point eq. (3)

Re_{PB} packed bed Reynolds number eq. (24)

Re_s particle Reynolds number based on relative velocity eq. (13)

S   mass flux of flowing solids, $kg/(m^2 s)$

t   time, s

u_g superficial gas velocity, m/s

u_g' effective superficial gas velocity, $(=u_g/(\varepsilon-\beta))$, m/s

$u_{g,corr}$ corrected superficial gas velocity, eq. (7), m/s

u_g relative velocity between gas and flowing solids, m/s

$\overline{u}_R$ mean relative velocity, m/s

u_{Rt} terminal relative velocity, m/s

u_s particle velocity, m/s

$\overline{u}_s$ mean particle velocity, m/s

u_{sL} local mean particle velocity, eq. (29), m/s

u_{st} terminal particle velocity, m/s

v volumetric flow rate of tracer particles, m^3/s

v_{dyn} volumetric flow rate of tracer particles through mixed tanks, m^3/s

v_{st} volumetric flow rate of tracer particles plug flow units, m^3/s

V_c bed volume, m^3

V_{dyn} volume of ideally mixed unit (dynamic zone), eq. (30), m^3

x_{dyn} fraction of tracer particles in the ideally mixed unit, eq. (30)

x_{st} fraction of tracer particles at the exit of the plug flow unit, eq. (31)

y_{dyn} fraction of dynamic solids flow rate, $(=v_{dyn}/v)$

y_{st} fraction of static solids flow rate, $(=v_{st}/v)$

z   axial coordinate along the packed bed column, m

β flowing solids holdup

β_{dead} dead part of static solids holdup ("dead zone")

β_{dyn} dynamic solids holdup

β_{st} static solids holdup

$\Delta p/L$ pressure drop per fixed bed length, Pa/m

ε fixed bed void fraction

ε_{corr} corrected fixed bed void fraction open to gas flow $(=\varepsilon-\beta)$

ε_{tr} void fraction in solids trickles, eq. (7)

γ relative pressure drop, eq. (25)

ϕ fraction of tracer in static solids holdup

φ fraction of tracer in active part of static solids holdup

μ gas dynamic viscosity, $kg/(m \cdot s)$

θ_{dyn} dimensionless time for ideally mixed tank: $(=t/\tau_{dyn})$

θ_R ratio between time delay and space time $(=\tau_{st}/\tau_{dyn})$

ρ_g gas density, kg/m^3

ρ_s skeletal density of the flowing solids particles, kg/m^3

τ_{dyn} space time in ideally mixed tanks in series, s

τ_{st} time delay in plug flow (time delay of flowing solids), eq. (31), s

ψ empirical parameter, eq. (18)

LITERATURE

[1] De Directie Van De Staatsmijnen in Lumburg. French Patent 978287, 1948.

[2] Kaveckii, G.D.; Planovskii, A.N. Khim. Tekhnol. Topl. Masel. **11** (1962) 8.

[3] Claus, G., Vergnes, F., Le Goff, P. Can. J. Chem. Eng. **54** (1976) 143.

[4] Roes, A.W.M., Van Swaaij, W.P.M. Chem. Eng. J. **17** (1979) 81.

[5] Large, J.F., Naud, M., Guigon, P. Chem. Eng. J. **22** (1981) 95.

[6] Verver, A.B., Ph. D. Thesis, University of Twente, Enschede, The Netherlands, 1984.

[7] Saatdjian, E., Large, J.F. Chem. Eng. Sci. **40** (1985) 693.

[8] Verver, A.B., Van Swaaij, W.P.M. Powder Technol. **45** (1986) 119.

[9] Westerterp, K.R., Kuczynski, M. Chem. Eng. Sci. **42** (1987) 1539.

[10] Kiel, J.H.A., Ph. D. Thesis, University of Twente, Enschede, The Netherlands, 1990.

[11] Duduković, A.P., Predojević, Z.J., Petrović, D.Lj, Pošarac D., J. Serb. Che. Soc. **57** (1992) 309–317.

[12] Benali, M., Shakourzadeh–Bolouri, K., Large, J.F. Proc. Found. Conf. Fluid., 7th (1992) 651–658.

[13] Benali, M., Shakourzadeh–Bolouri, K., Int. J. Multiph. Flow **20** (1994) 161.

[14] Predojević, Z.J., Ph.D. Thesis, Faculty of Technology, Novi Sad, Yugoslavia, 1997.

[15] Predojević, Z.J., Petrović, D.Lj., Duduković, A.P. Chem. Eng. Commun. **162** (1997) 1.

[16] Predojević, Z.J., Petrović, D.Lj., Martinenko, V., Duduković, A.P., J. Serb. Chem. Soc. **63** (1998) 85.

[17] Stanimirović, O.P., B.S. Thesis, Faculty of Technology, Novi Sad, Yugoslavia, 1998.

[18] Pjanović, R.M., S. Thesis, Faculty of Technology and Metallurgy, Belgrade, Yugoslavia, 1998.

[19] Predojević, Z.J., Petrović, D.Lj., Duduković, A.P., Ind. Eng. Chem. Res. **40** (2001) 6039.

[20] Nikačević, N.M., Duduković, A.P., Predojević, Z.J., J. Serb. Chem. Soc. **69** (2004) 77.

[21] Barysheva, L.V., Borisova, E.S., Khanaev, V.M., Kuzmin, V.A., Zolotarskii, I.A., Pakhomov, N.A., Noskov, A.S. Che. Eng. J. **91** (2003) 219–225.

[22] Guigon, P., Large J.F., Molodstof, Y. In Encyclopedia of Fluid Mechanics, Cheremissinoff, N, Gulf Publishing Co.: Houston, 1986, 1185.

[23] Kiel, J.H.A., Van Swaaij W.P.M. AIChE Symp. Ser. **85** (1989) 11–21.

[24] Duduković, A.P., Nikačević, N.M., Petrović, D.Lj., Predojević, Z.J. Ind. Eng. Chem. Res. **42** (2003) 2530.

[25] Duduković A.P., Nikačević N.M., Kuzeljević Ž.V., Ind. Eng. Chem. Res, **43** (2004), 7445.

[26] Turton, R., Levenspiel, O. Powder Technol. **47** (1986) 83.

[27] Duduković A.P., Nikačević N.M., Pjanović R.V., Kuzeljević Ž.V., J. Serb. Chem. Soc. **70** (2005) 137–144.

[28] Nikačević N.M., Duduković A.P., Ind. Eng. Chem. Res. **44** (2005), 6509.

[29] Roes, A.W.M., Van Swaaij, W.P.M., Chem. Eng. J. **18** (1979) 13.

[30] Roes, A.W.M., Ph.D. Thesis, Twente University of Technology, The Nederlands, 1978.

[31] Compagnie de Saint–Gobain. French Patent 1469109, 1965.

[32] Verver, A.B., Van Swaaij, W.P.M. Powder Technology **45** (1986) 119.

[33] Boumehdi, P., Guigon, P., Large J.F. Heat Recovery Systems **5** (1985) 407–414.

[34] Le Lan, A., Niogret, J., Large, J.F., McBridge, J.A. AIChE Symp. Ser. **80** (1984) 110–115.

[35] Roes, A.W.M., Van Swaaij, W.P.M. Chem. Eng. J. **18** (1979) 29.

[36] Kiel, J.H.A., Prins, W., Van Swaaij, W.P.M Chem. Eng. Sci. **48** (1993) 117.

[37] Westerterp, K.R., Kuczynski, M.A. Hydrocarbon Processing, Int. Ed. **65** (1986) 80–83.

[38] Westerterp, K.R., Bodewes, T.N., Vrijiland, M.S., Kuczynski, M.A. Hydrocarbon Processing, Int. Ed. **67** (1988) 69–73.

[39] Kuczynski, M., Oyevaar, M.H., Pieters, R.T., Westerterp, K.R. Chem. Eng. Sci. **42** (1987) 1887.

[40] Westerterp, K.R., Kuczynski, M., Chem. Eng. Sci. **42** (1987) 1871.

[41] Verver, A.B., Van Swaaij, W.P.M. Institution of Chemical Engineers Symposium Series 87 (Chem. React. Eng) (1984) 177–184.

[42] Kiel, J.H.A., Prins, W., Van Swaaij, W.P.M. Chem. Eng. Sci. **47** (1992) 4271.

[43] Duduković A.P., Nikačević N.M., Chapter 22 In Finely Dispersed Particles: Micro–, Nano–, and Atto–Engineering (editors: Aleksandar Spasić, Jyh–Ping Hsu), CRC Taylor and Francis, Inc., USA, 2005, 567–600.